

## Amplitude modulation of atomic wave functions

Xiao Wang and W. E. Cooke

Department of Physics, University of Southern California, Los Angeles, California 90089-0484

(Received 6 December 1991; revised manuscript received 10 July 1992)

When a two-electron-like atom has one electron excited to a Rydberg state, and the other electron is then excited for a time that is short compared to the orbit time of the Rydberg electron, a “notch” is created in the Rydberg wave function, corresponding to that part which autoionized during the small time that the core was excited. This notch is initially localized in space and momentum, and follows a classical trajectory in momentum space. This transient-core-excitation method is a very efficient way to create notched atomic wave functions, and is demonstrated here using a long pulse core excitation.

PACS number(s): 31.50.+w, 32.90.+a

When a Rydberg state of a two-electron-like atom is excited to an autoionizing Rydberg state [1] by a short-pulse core excitation, a shock wave is generated in the Rydberg electron's wave function [2]. The core electron's dipole moment in this doubly excited state then decays in a classical fashion, in a series of “stair steps” [3]. Although the net decay of the autoionizing state is still nearly exponential, the “stair-step” behavior is somewhat reflected in that part of the Rydberg wave function localized near the core electron [2]. Here, we show that a short-pulse core excitation, followed by a second short-pulse core *deexcitation* can capture that behavior and produce a “dark-wave” packet [4, 5] in the bound Rydberg electron's wave function *in momentum space*. This means that the momentum-space wave function has a localized depletion and that this depletion follows a classical trajectory. This is the complement to the normal Rydberg wave packet, which is created by short excitation pulses [6, 7]. The very high efficiency of this process should make it possible to modify a Rydberg wave function *arbitrarily*, to generate almost any desired wave-function amplitude envelope. We illustrate the characteristics of this unusual excitation by illustrating the time evolution of the wave function in momentum space and by decomposing the wave function into Rydberg states of well-defined principal quantum number  $n$ . We report experimental evidence of this process by observing this redistribution into other bound states of different principal quantum number.

Consider a two-electron-like atom (e.g., barium) where one electron is in a bound Rydberg state of principal quantum number  $n$ , and the other (which we will call the “core” electron) is in its ground electronic state. This state has a binding energy of  $W_n = -0.5/n^{*2}$ , where  $n^*$  is called the effective quantum number. If the core electron is excited with a short laser pulse, then the core transition itself can “shake up” the Rydberg electron into a variety of different states, with new effective quantum numbers  $\nu$ . The transition moment for this process is proportional to a factor representing the energy density of doubly excited states and the overlap integral between initial and

final Rydberg states,  $\langle n|\nu \rangle$  [1]. The quantum number  $\nu$  and the energy become continuous variables, since doubly excited states are so short lived. With this excitation, the time-dependent Rydberg wave function of the doubly excited state can be written as

$$|\Psi\rangle \propto \int |A_\nu|^2 e^{-iW_\nu t} |\nu\rangle \langle \nu|n\rangle dW_\nu, \quad (1)$$

where  $|A_\nu|^2$  is the aforementioned energy density of doubly excited states, and the Rydberg overlap factor can be written as

$$\langle \nu|n\rangle = \frac{\sin \pi(n^* - \nu)}{\pi(W_n - W_\nu)}. \quad (2)$$

This wave function looks just like the original Rydberg wave function  $|n\rangle$ , at  $t = 0$ ; however, as time evolves, the incoming wave-function flux is partially autoionized, so that less flux leaves the small- $r$  region. This generates a shock wave that propagates along a classical trajectory [2].

But, if a second pulse is applied after a delay time  $t_d$ , then the autoionizing Rydberg wave function will be projected back onto the original, bound Rydberg series. The final, time-dependent, *bound*, wave packet thus becomes a discrete sum over the bound states. Again, this may result in a net change in principal quantum number as a result of the first and the second shake process. The coefficient of excitation into each state,  $m \neq n$ , can be written as

$$c_m \propto \int |A_\nu|^2 \langle n|\nu\rangle \langle \nu|m\rangle e^{-iE_\nu t_d/\hbar} dE_\nu, \quad (3)$$

where we have omitted an overall normalization factor that depends on the length and strength of the excitation pulses.

Since this two-step process can result in a *different* bound Rydberg state, it is relatively easy to detect such shake transitions. Selective field ionization [8] has routinely been used to detect relative populations in bound

Rydberg states over a wide range of quantum numbers. The characteristics of the final-state distribution will have some simple, general behaviors.

For example, if the doubly excited states form a single

Rydberg sequence, coupled to a single continuum, then standard expressions can be used for the density of states and the overlap factor [9] so that the coefficients can be written as

$$c_m = \int \frac{\sinh(\pi\gamma/2)}{|\sin[\pi(i + \delta + i\gamma/2)]|^2} \frac{\sin[\pi(n^* - \nu)]}{\pi(W_n - W_\nu)} \frac{\sin[\pi(m^* - \nu)]}{\pi(W_m - W_\nu)} e^{-iW_\nu t_d} dW_\nu. \quad (4)$$

To the extent that the bound series is unperturbed so that  $m - n$  is an integer and the spacing between adjacent states does not vary much from one state to the next, then each  $c_m$  for  $m \neq n$  can be factored into a normalization factor  $f(t_d)$  times an  $m$ -dependent modulation:

$$c_m = (-1)^{n-m} \frac{\sin[\frac{1}{2}(W_m - W_n)t_d]}{\frac{1}{2}(W_m - W_n)} e^{-iW_n t_d} f(t_d). \quad (5)$$

Figure 1 shows the squares of the coefficients for the  $n = 47, 48$ , and  $49$  states as a function of  $t_d$ , obtained by integrating Eq. (4). The initially excited Rydberg state was an  $n = 45$  state. For the doubly excited autoionizing states, we used  $\gamma = 0.1$ ,  $\delta = 0.5$ ; however, this only affects the stair-step normalization envelope. Clearly, it is possible to construct unusual  $m$ -state distributions by choosing the delay time  $t_d$  appropriately. Note, for example, that near  $t_d = 0.5$  Rydberg cycles, mostly states where  $m - n$  is odd will be excited.

These Rydberg wave packets are most instructive in a pseudomomentum space. We have numerically integrated Eq. (1) to obtain spatial wave functions using a scaled radial coordinate  $u = \sqrt{r/2}$ . This scaling changes the wave function to  $\chi(u) = r^{3/4}R(r)$ , where  $R(r)$  is the usual Rydberg radial wave function. The net effect of these scale changes is to compress the extent of the wave function [2] and to force it to look more like a harmonic-oscillator function. We then Fourier transformed these functions to obtain a picture of the packet

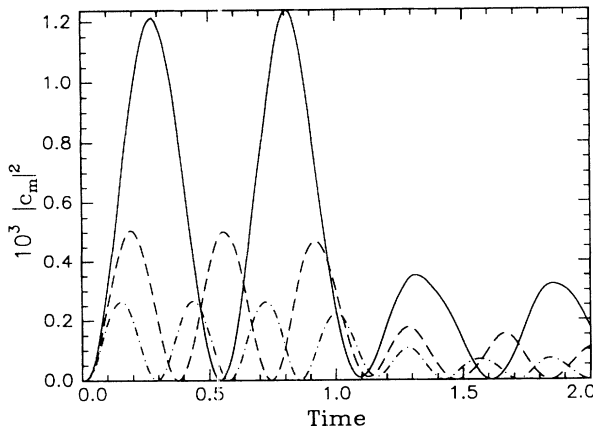


FIG. 1. Relative population shaken into  $m = 47$  (solid),  $m = 48$  (dashed), and  $m = 49$  (dashed-dotted) states as a function of the delay time (in units of Rydberg cycles) between the excitation and deexcitation pulses. The initial Rydberg state was an  $n = 45$  state.

in momentum space, where  $p = i\partial/\partial u$ .

Figure 2 shows the square of the complex amplitude of these wave functions in momentum space and how they develop in time, where we have chosen  $t_d = 0.2$  and have characterized the autoionizing states by  $\gamma = 0.3$  and  $\delta = 0.5$ . In this sequence it is clear that a notch has developed in the momentum profile, at the end representing high-momentum outgoing waves. These waves are those which passed through the core region while it was excited and thus partially autoionized. As time progresses, this notch traverses to lower momentum (corresponding to large radial coordinate values), and then to large negative momentum values (corresponding to small radial coordinates, *approaching* the core). The width of this notch is proportional to the delay time between the two pulses, and the depth of the notch depends primarily on the rate of autoionization of the doubly excited state. The notch is not as clear in  $u$  space as in  $p$  space because the wave function is constructed from waves traveling in both directions. These two waves tend to blur the notch, except for when the notch occurs at a turning point.

In our experiments, we have used a single pulse to ex-

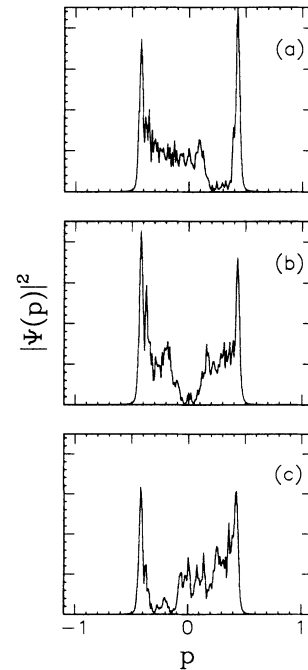


FIG. 2. Time evolution of a notch in the momentum wave function. The square of the momentum wave functions is plotted for times of 0.05, 0.4, and 0.7 Rydberg cycles after the excitation, in (a), (b), and (c), respectively.

cite and deexcite the core electron. Our pulses are fairly long (nanoseconds), and would require  $n$  values in excess of 300 to examine the timing details. Such states are exceedingly fragile. Consequently, we have examined  $6snd$  states in the vicinity of  $n = 130$ , where the Rydberg electron makes several orbits during a laser pulse. "Notching" still occurs in this case, since our laser has considerable excess bandwidth and the beating of its many modes creates a series of pulses shorter than a Rydberg orbit period. This series of pulses is not repeatable, or controllable, so we have restricted our measurements and *only* observe the population redistribution that accompanies "notching."

We used standard two-color, stepwise excitation of an atomic beam of barium to prepare the initial bound states. The excitation region is between two parallel capacitor plates separated by 2.5 cm. The top plate is electrically grounded, but has a hole in the center, covered with a screen, so that electrons may leave the interaction region. To analyze the state composition, we applied a small negative voltage ramp to the bottom plate. In this way, a state is identified by the field required to ionize it, since this determines the time that the electron takes to arrive at the detector. We detected electrons with a microchannel-plate particle detector placed 3 cm above the interaction region. The field between the capacitor plates is nominally kept at zero during the bound states' excitation; however, these states are extremely susceptible to even the smallest fields. We estimated the residual field to be less than 100 meV/cm by monitoring the collection of photoionization electrons as we varied a dc bias. For the wrong sign bias, no electrons reach the detector. Nevertheless, the small Stark field will mix the  $l$  states near  $n = 130$ , so we have initially excited a band of Stark states, rather than states of well-defined  $l$  value. This does not destroy the notching process, since all the  $l$  states have the same radial orbit period [10]. (Although, the mixing will reduce the autoionization efficiency and change the phase shift due to the elastic interactions between the Rydberg and core electrons.) Our Rydberg excitation laser had a bandwidth of less than  $0.2 \text{ cm}^{-1}$  (as measured using an air-spaced étalon with a free spectral range of  $0.8 \text{ cm}^{-1}$ ), so that it excited a relatively narrow band of Rydberg states.

The field required to ionize a Rydberg state is  $3.3(100/n)^4 \text{ V/cm}$ , and this decreases rapidly with increasing  $n$  values. Thus, when the ionization field is ramped, higher- $n$  states ionize at earlier times, when the field is still low. Our field-ionization ramp has a rise time of approximately  $1.5 \mu\text{s}$ , and the pulse is applied approximately  $1.5 \mu\text{s}$  after the state excitation. This allows double discrimination in the state analysis, since the peak ionization field *and* the electron arrival time can be set.

We typically set our field-ionization voltage pulse 30 meV below threshold ( $\sim 1 \text{ V/cm}$ ), and swept a 493-nm-wavelength laser near the core electron  $6s \rightarrow 6p_{1/2}$  transition. The core laser has a pulse length of approximately 3 ns, a bandwidth of  $\approx 0.8 \text{ cm}^{-1}$  (which is due to many longitudinal modes in the oscillator), and arrives approximately 20 ns after the bound Rydberg states are

prepared. We detected our signal with a boxcar integrator, whose gate could be set to detect the prompt signal showing electrons produced by autoionization or to detect the delayed signal that showed electrons produced by the field ionization of *higher* bound states than those initially excited. Figure 3 shows traces of a storage oscilloscope, with a retention time of 5 s (approximately 50 laser pulses). The top trace shows the ionizing field produced by a voltage pulse on the lower plate. The center trace shows the field-ionization signal without the core laser present and with the ionization field set *just above the field-ionization threshold*. The first structure is the rf noise from the laser  $Q$  switch, followed by more rf noise when the ionizing ramp begins, approximately  $1.5 \mu\text{s}$  later. As the ionization ramp rises, it reaches the threshold for Rydberg ionization, and the resulting electrons begin with a sharp threshold. The bottom trace shows the ionization signal *with the core laser present*. Direct photoionization arrives promptly, with the  $Q$ -switch rf noise. Field ionization of the original Rydberg population (and any redistribution into higher states) is still present. The new feature — electrons arriving at significantly lower ionization threshold — demonstrates that the core laser has produced the redistribution into lower states, which is indicative of "notching" the Rydberg wave function. The storage-oscilloscope traces have been heavily saturated at times greater than  $3 \mu\text{s}$ , so this figure shows more apparent redistribution than actually occurs. On a single laser pulse, five events can usually be seen at the low fields, with the high-field events overlapping as in the figure.

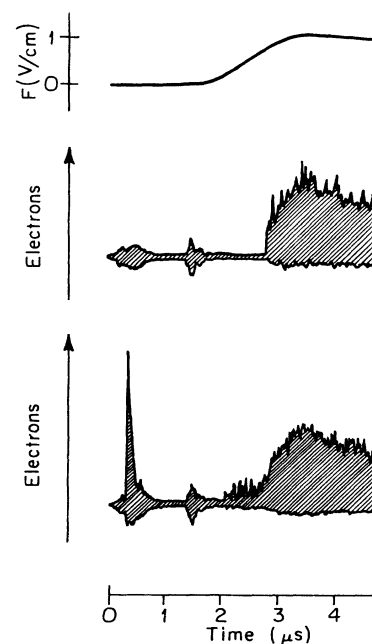


FIG. 3. Storage-oscilloscope traces of approximately 50 laser pulses. The top trace shows the ionization field. The center trace shows the field-ionization signal without the core excitation. The bottom trace shows the ionization signal with the core-laser driving transitions to generate the redistribution.

Figure 4 shows how the photoionization signal and the “shake” vary with core-laser tuning, when the core laser fluence is low ( $\sim 10 \mu\text{J}/\text{cm}^2$ ). Each point corresponds to the average of four separate sweeps (a sweep sums data during 30 laser pulses), and the error bars show the standard deviation of those four sweeps.

The shake signal is asymmetric, showing less signal to the low-energy side. At these low-energy detunings of the core laser, the excitation produces a “shake” into lower  $n$  states to conserve energy. However, since the core laser power is low, the transitions back to the bound-state spectra occur primarily from *spontaneous* core fluorescence, very near the ionic transition frequency. This is yet another illustration of the efficiency of this process, that the *vacuum* fields are sufficiently strong to drive the shake transitions. The net effect is to *lower* the principal quantum number of the bound state, so that it will not be ionized by a field that can ionize the initial state. Moreover, these notching transitions *will not* increase with the square of the laser intensity as a normal two-photon transition, because at low intensities, the second transition is dominated by *spontaneous* fluorescent decay of the core electron [11], rather than by laser-induced transitions.

At higher core-laser powers, the transition back to the bound state is dominated by *stimulated* transitions that occur near the laser frequency. These stimulated transitions bring the atoms back to a band of bound states within the laser linewidth of the original state, independent of the laser frequency detuning. These are the two-step transitions we have described above. At higher fluences of  $\sim 100 \mu\text{J}/\text{cm}^2$ , the photoionization and shake signals thus look identical because the ionic core transition has been saturated.

We currently do not have the ability to observe *shake-down* into lower states, since the electrons from lower states arrive just after the large signal from atoms, which remain near the initial  $n$  value. However, by examining the field-ionization range of the atoms making transitions to higher  $n$  states, we have determined that the shake

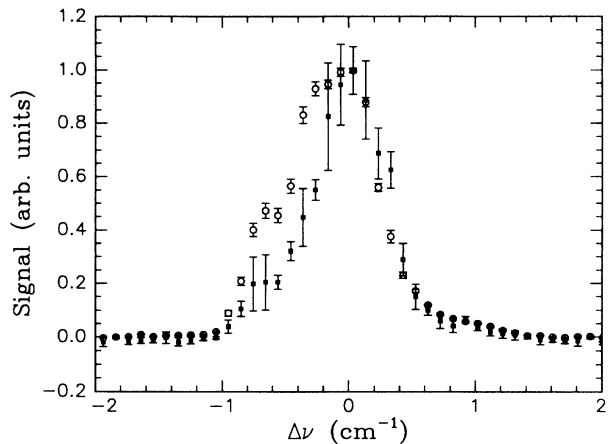


FIG. 4. Photoionization (circles) and shake signal into higher- $n$  states (squares) as a function of core-laser detuning from the ionic transition. Error bars show standard deviation from four separate sweeps.

transitions produce  $n$  values shifted by 5 or 10. This is consistent with our laser linewidth.

This core excitation method is a very efficient method to “notch” Rydberg momentum wave functions, creating dark waves. Dark waves have been discussed as a product of extremely high fields stabilizing Rydberg electrons [4]; however, the fields suggested here are very modest. If one were to use a shorter pulse laser, then it should be possible to impose arbitrarily shaped timing notches on a wavefunction. Even with 1-ps-long laser pulses, the saturation fluence should be less than  $10 \text{ mJ}/\text{cm}^2$ , so that currently available laser systems should be able to create significant quantities of such notched atoms.

This work was supported by the National Science Foundation under Grant No. PHY88-14903.

- [1] W.E. Cooke, T.F. Gallagher, S.A. Edelstein, and R.M. Hill, Phys. Rev. Lett. **41**, 178 (1978); S.A. Bhatti, C.L. Cromer, and W.E. Cooke, Phys. Rev. A **24**, 161 (1981); N.H. Tran, P. Pillet, R. Kachru, and T.F. Gallagher, *ibid.* **29**, 2640 (1984).
- [2] Xiao Wang and W.E. Cooke, Phys. Rev. A (to be published).
- [3] Xiao Wang and W.E. Cooke, Phys. Rev. Lett. **67**, 976 (1991).
- [4] M.V. Federov, M. Yu Ivanov, and P.B. Lerner, J. Phys. B **23**, 2505 (1990).
- [5] K. Burnett, P.L. Knight, B.R.M. Piraux, and V.C. Reed, Phys. Rev. Lett. **66**, 301 (1991).
- [6] J. Parker and C.R. Stroud, Jr., Phys. Rev. Lett. **56**, 716 (1986); J. A. Yeazell, M. Mallalieu, J. Parker, and C. R. Stroud, Jr., Phys. Rev. A **40**, 5040 (1989).
- [7] A. ten Wolde, L.D. Noordam, H.G. Muller, A. Legendijk, and H.B. van Linden van den Heuvell, Phys. Rev. Lett. **61**, 2099 (1988).
- [8] T.W. Ducas, M.G. Littman, R.R. Freeman, and D. Kleppner, Phys. Rev. Lett. **35**, 366 (1975); T.F. Gallagher, L.M. Humphrey, R.M. Hill, and S.A. Edelstein, *ibid.* **37**, 1465 (1976); T.H. Jeys, G.W. Foltz, K.A. Smith, E.J. Beiting, F.G. Kellert, F.B. Dunning, and R.F. Stebbings, Phys. Rev. Lett. **44**, 390 (1980).
- [9] W.E. Cooke and C.L. Cromer, Phys. Rev. A **32**, 2735 (1985).
- [10] John A. Yeazell and C. R. Stroud, Jr., Phys. Rev. A **35**, 2806 (1987); John A. Yeazell and C. R. Stroud, Jr., Phys. Rev. Lett. **60**, 1494 (1988).
- [11] A. Lindgard and S.E. Nielsen, At. Data Nucl. Data Tables **19**, 533 (Academic, New York, 1977).